Available online at www.sciencedirect.com

ScienceDirect

Procedia Engineering 14 (2011) 1266–1274

Procedia Engineering

www.elsevier.com/locate/procedia

The Twelfth East Asia-Pacific Conference on Structural Engineering and Construction

Plastic Hinge Length in Reinforced Concrete Flexural Members

Xuemei Zhao[1a], Yu-Fei Wu[1b], A.Yt. Leung[1] and Heung Fai Lam[1]

[1]*Department of Building and Construction, City University of Hong Kong, China*

Abstract

For reinforced concrete (RC) flexural members, the plastic deformation is localized in a small zone namely the plastic hinge zone after the yielding of the member. The performance of the plastic hinge zone is critical for flexural members as it governs the load carrying and deformation capacities of the member. Therefore, plastic hinge has been of great interest to structural designers and researchers for decades. The length of the plastic hinge zone is an important design parameter where intense confinement should be provided to increase the ductility of the member for survival from extreme events such as earthquakes. The behavior of plastic hinges is very complicated due to the high nonlinearity of materials, interaction and relative movement between the constituent materials, and strain localization. As a result, most researchers investigated the problem through experimental testing. Restricted by the time and cost involved in large tests, very limited knowledge has been obtained up to date. This work tries to investigate the problem analytically with Finite Element Method (FEM) using the computational software DIANA. A computational model is built and verified with existing experimental data including load deflection response, rotational capacity, and strain and stress distributions of reinforcement. With the calibrated FEM model, the extent of the rebar yielding zone, concrete crush zone, curvature localization zone and the real plastic hinge length are studied. Parametric studies are subsequently employed to investigate the plastic hinge length in terms of material properties of rebar and concrete, dimensions of the member, and reinforcement ratio.

Keywords: Plastic hinge length, Finite Element Analysis, reinforced concrete, beam, DIANA

[a] Presenter: Email:: zhao.xm@student.cityu.edu.hk

[b] Corresponding author: Email: yfwu00@cityu.edu.hk

1877–7058 © 2011 Published by Elsevier Ltd. Open access under CC BY-NC-ND license.
doi:10.1016/j.proeng.2011.07.159

1. Introduction

For decades the plastic hinge where plastic deformation is concentrated has been an interesting and complicated research subject of RC members. The performance of plastic hinge is critical to the member's load carrying and deformation capacities. Although numerous empirical equations have been proposed for the prediction of the plastic hinge length L_p as summarized in Table 1, the accuracy of L_p remains an open issue to be addressed. The combination of three phenomena, namely, the high concentration of compression strain around the section of maximum moment that complicates the notion of base curvature, the tension shift that invalidates the assumption that plain sections remain plane, and the strain penetration that results in a fixed end rotation at the base of columns, explains the difficulties of the problem (Hines et al. 2004).

The plastic hinge length L_p in Table 1 is not the physical length of the real plastic hinge region, $L_{pc,}$ over which actual plasticity spreads. Instead, it is an equivalent length over which a given plastic curvature is assumed to be constant for the integration of cross-sectional curvatures along the RC member length to solve the member's flexural deflection and plastic rotation capacity (Park and Paulay 1975). Nevertheless, L_{pc} is logically believed to have certain intimate relationship with L_p. Thus, L_{pc} over which intense confinement should be provided is not only important for prevention of damage from extreme events such as earthquakes, but also interesting for prediction of L_p. However, the high nonlinearity of materials and interactions and relative movements between the constituent materials in the plastic hinge zone greatly complicate the problem. As a result, the studies of plastic hinges in RC members are so far limited to experimental testing. However, the traditional way to investigate the problem through experimental testing is restricted by the time and cost involved in large tests. As finite element (FE) analyses become more and more mature and with rapid increase in computer speed, this work tries to investigate the plastic hinge region of RC members through FE numerical simulations.

Table 1: Empirical expressions for plastic hinge length

Researcher Reference	Plastic Hinge Length Expression (l_p)
Baker (1956)	$k(z/d)^{1/4}d$ (for RC beams and columns)
Sawyer (1964)	$0.25d+0.075z$
Corley (1966)	$0.5d+0.2\sqrt{d(z/d)}$ (for RC beams)
Mattock (1967)	$0.5d+0.05z$ (for RC beams)
Priestlley and Park (1987)	$0.08z+6d_b$ (for RC columns)
Paulay and Priestley (1992)	$0.08z+0.022d_bf_y$ (for RC beams and columns)
Sheikh and Khoury (1993)	$1.0h$ (for columns under high axial loads)
Coleman and Spacone (2001)	$G_f^c/\left[0.6f_c^{'}(\varepsilon_{20}-\varepsilon_c+0.8f_c^{'}/E_c)\right]$
Panagiotakos and Fardis (2001)	$0.18z+0.021d_bf_y$ (for RC beams and columns)
Bae and Bayrak (2008)	$l_p/h=[0.3(p/p_o)+3(A_s/A_g)-1](z/h)+0.25\geq 0.25$ (for columns)

Note: A_g= gross area of concrete section; A_s =area of tension reinforcement; d =effective depth of beam or column; d_b =diameter of longitudinal reinforcement; E_c =Young modulus of concrete; f_c =concrete compressive strength; f_y= the yielding stress of reinforcement;

G_f^c =concrete fracture energy in compression; h =the overall depth of beam or column; p=applied axial force;

$p_o=0.85f_c^{'}(A_g-A_s)+f_yA_s$ =nominal axial load capacity as per ACI 318-05 (2005);

z =distance from critical section to point of contraflexure; ε_c =peak compressive strain;

ε_{20}=strain corresponding to 20% of the compressive strength

2. Finite Element Modeling and Implementation

The commercial software DIANA is employed for the FE simulations in this work. For simply supported beams, only half of the beam is modeled for simplification. As half of the simply supported beam is geometrically identical to a cantilever column, the model is also applicable to columns. Two-dimensional model and monotonic loading are investigated in this work, and the Arc-length method is used for numerical solution.

2.1. Modeling of concrete

The three-node triangular isoparametric plane stress element is adopted for the concrete elements in the study. The mesh size is generally to be 10 - 20 mm which is close to the size of the aggregate. Mander's stress-strain model (Mander et al. 1988) is adopted for both confined and unconfined concrete.

2.2. Modeling of reinforcing steel

The regular truss element in DIANA is employed for modeling of reinforcing bars. Ideal plasticity model according to NEN 6770 code is employed to model the material property of the reinforcing steel and where applicable strain hardening effect is taken into account. Compressive steels are modeled as embedded reinforcement elements.

2.3. Modeling of bond-slip relationship

The structural interface element L8IF given by DIANA is adopted for modeling the interface between concrete and the reinforcing steel. A typical 4-segment envelop in accordance with the CEB-FIP Model Code 1990 is employed to model the bond stress-slip relationship between concrete and the reinforcing steel in this study.

3. Numerical Model Verification

Five experimentally tested specimens are modeled in this section to validate the FE model in several respects. As shown in Table 2, these specimens were tested by different researchers. Consequently, from the statistical and sampling point of view, the FE model and the corresponding procedure verified by these test results are considered well validated.

Table 2: Properties of the test units

Specimen (reference)	f_c, MPa	f_t, MPa	E_c, GPa	f_y, MPa	E_s, GPa	d,mm	b,mm	z,mm	Tension steel d_b ,mm x No.s
B1 (Au and Bai 2007)	52	4.5	27	488	200	260	200	1300	16x3
A2 (Mattock 1965)	42.3	3.45	21	318	195.8	254	152	1398	19x2
B15 (Mainst 1952)	28.8	2.84	26.8	433	213.7	254	203	530	22.2x1
C1 (Scott 1996)	49.9	3.3	31.4	382	207	175	110	850	12x2
C1A (Scott 1996)	60	3.65	34.5	382	207	175	110	850	12x2

3.1. Verification of load deflection response

Specimen B1 is a simply supported beam under three-point bending. Details of the beam are listed in Table 2 in which b is the width of the beam. From Fig. 1, good agreement is observed between the FE numerical results by the author and by Au and Bai as well as the test results.

3.2. Verification of rotational capacity

Curvature and rotation are of particular interest in the plastic hinge region. In the study, numerical results of curvature ϕ and rotation θ are not direct outputs from the FE analyses, but calculated with Equations (1) and (2) respectively.

$$\phi = \frac{\Delta_t - \Delta_c}{hL_g} \tag{1}$$

$$\theta = \frac{\Delta_t - \Delta_c}{h} \tag{2}$$

where Δ_t = extension at tension face along a length of L_g, Δ_c = shortening at compression face along a length of L_g. .

Specimen A2 is also a simply supported beam under three-point bending. The hardening of steel is considered in FE model as test data of the stress strain relationship is available.

According to Mattock, the rotation at the mid-span was measured in a length of beam equal to its effective depth d and calculated from the measured shortening and extension at the top and bottom of the section of the beam. To be comparable, L_g in the numerical calculation is taken as or closest to d. Detailed comparison is given in Table 3 for the deflection Δ, corresponding lateral applied load F, and curvature ϕ at yield and ultimate of specimen test respectively. Test data of rotation θ is available at ultimate only, and only this value is compared. Generally good agreements with test results are observed except the numerical ϕ_u is much bigger than the test result, but this test result is in fact not the ultimate value because of damage of sensors and this explains the big deviation.

Table 3: Comparison for numerical and test results from A2

Specimen A2	Δ_y, mm	F_y, mm	Δ_u, mm	F_u, mm	$_y$, μrad/mm	$_u$, μrad/mm	θ_u
Numerical result	6.43	35.3	119	45.06	9.06	288	0.0732
Test result	9.5	32	102.4	45	11	177+	0.0627
Numerical result/Test result	0.68	1.1	1.16	1	0.82	1.63	1.167

Note: A + sign indicates this was the last reading obtained. Subscript $_y$ is at the moment of yielding of the tension reinforcement;

$_u$ is the instant at which the maximum load on the beam is reached under increasing load or the beam fails after some time at constant load.

3.3. Verification of strain and stress distribution of reinforcing steel

The strain distribution of reinforcing steel is with no doubt critical for gaining insight into the intrinsic mechanism in plastic hinge region. However, it is rather difficult to obtain reliable data from test as the measurement technique must not affect the bond between the bars and the surrounding concrete. To have persuasive verification, test specimens conducted with technique of installing strain gages in a machined duct running through the center of the reinforcement (Mainst 1952; Scott 1996) are adopted for FE

analyses and comparison. B15 is a simply supported beam under four-point loading. Steel hardening effect is also considered in the FE model as test data of the stress-strain relationship is available. C1 and CIA are specimens of beam-column joints. Other details of the beams of these joints are shown in Table 2. Although only the beam sections are of interest in the study, the full FE model of the joint as a whole is generated to allow for strain penetration into the column. Steel hardening effect is also considered in the FE model.

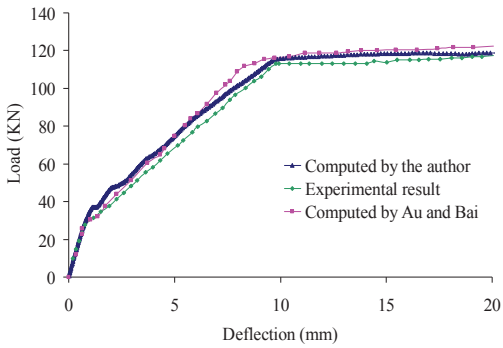

Fig. 1: Load Disp. curve of B1

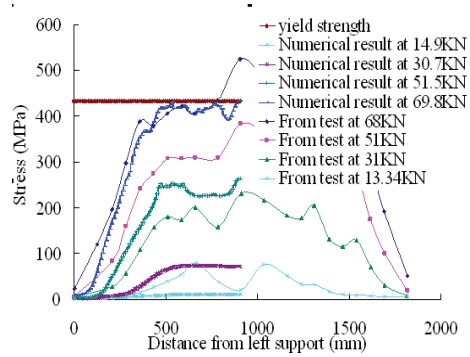

Fig. 2: Stress distribution of B15

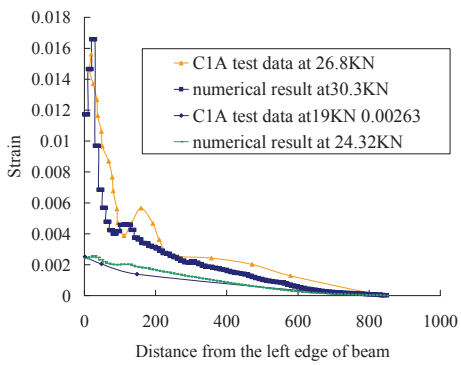

Fig. 3: Results of Column Beam Joint C1A

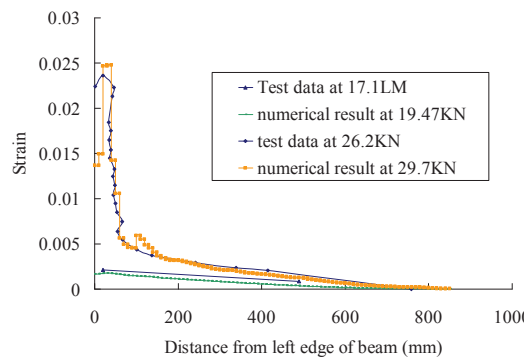

Fig. 4: Results of Column Beam Joint C1

Comparisons of test and numerical results for the steel strain distribution are given in Figures 2-4, in which numerical strain of the steel is compared with experimental result under the same or closest lateral load. For beam B15, experimental result of rebar strain is converted into rebar stress and compared with numerical result. Although individual magnitude of stress at a point may vary much from test result due to arbitrary cracks, the overall patterns of numerical stress distribution comply well with test results, especially after cracks occur. Better compliance with test results is obtained in the C1 and C1A simulations, from which steel strains are found to concentrate in a certain length from the maximum moment section after yielding of rebar.

4. Analyses with Calibrated Model

Plastic hinge region is closely related to the rebar yielding zone, concrete crushing zone and curvature localization zone where the curvature continues to increase while other parts maintain or reduce after the yielding of the member. These three interesting regions are thus investigated in details to get insight into the real plastic hinge zone in RC beams.

Investigation to the rebar yielding zone - The rebar yielding zone is defined as the region of the beam where the reinforcing steel in tension has reached or passed its yielding strength. It is observed from numerical simulations that although the length of this region varies as the loading steps continue to apply, the maximum length of the rebar yielding zone L_{ry} is still limited within a certain area and this length L_{ry} is investigated in parametric study. Further observation to rebar yielding zone shows that a clear fluctuation area of rebar strain forms after the rebar yields, or the concrete strain in compression side reaches 0.002, whichever occurs later, and interestingly in most of the cases this fluctuation zone tends to stop increasing after a certain loading step. Fig. 5 describes the maximum length of this fluctuation area L_{rc} and the length of the rebar strain concentration zone L_{ri} where large rebar strain increments are localized.

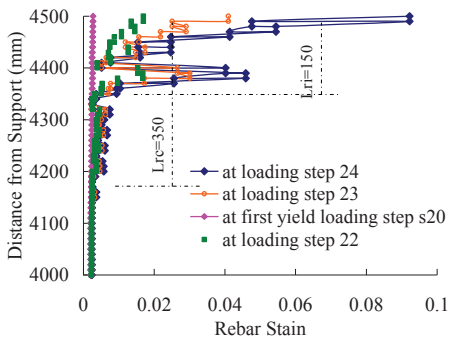

Fig. 5: Simulated rebar strain distribution

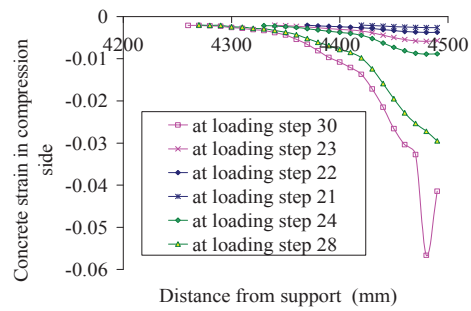

Fig. 6: Simulated concrete strain distribution

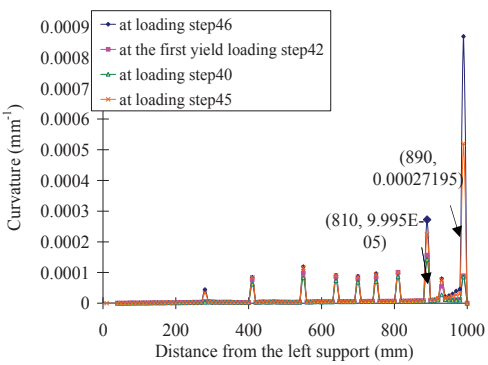

(a)

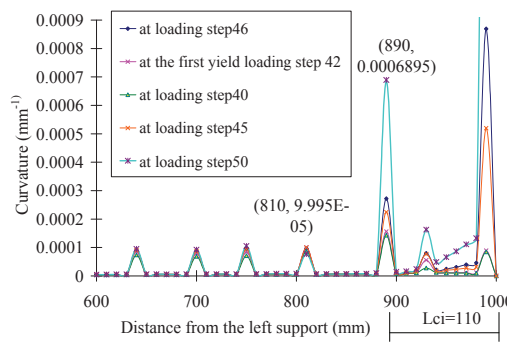

(b)

Fig. 7: Formation of curvature localization zone from FE analysis

Investigation to the concrete crush zone - To study the potential concrete crushing zone, the regions of the beam where the concrete strain in compression side is greater than 0.002 and where the concrete strain in compression side is greater than 0.006, are investigated. These regions extend as the loading step increases which trend is demonstrated in Fig. 6. The maximum lengths of these two regions, namely L_{c2} and L_{c6}, are investigated to locate the severe damage region of concrete.

Investigation to the curvature localization zone – Both from experimental tests and numerical simulations large curvature is found to concentrate in a certain area after the member yields, as shown by the numerical results from the study in Fig.7. The length of the curvature localization zone L_{ci} where the curvature continues to exhibit large increment under loading while other parts have little or no increment is found to be a constant for most of the cases.

5. Parametric Study

The following parameters are considered to be significant that affect the plastic hinge zone: the yielding strength of reinforcing steel f_y, the compressive strength of concrete f_c, the shear span of the beam z, the effective depth of the beam d, and the shear span over sectional depth ratio z/h. Parametric studies are undertaken to identify their effect to the various zones as defined in Section 4. The results of the parametric studies are given in Table 4, where the results are compared with the commonly used empirical formula $L_p = 0.08z$ and formulae from other researchers for beams. When a parameter is studied, all other parameters are fixed. Except for the parameter f_c which is investigated in a model without confinement, all other parameters are studied with confined models.

Table 4: Parametric studies

Parameter	Parametric value	L_{c2}	L_{c6}	L_{ry}	L_{rc}	L_{ri}	L_{ci}	$0.08z$	$L_{p,}$ Sawyer (1964)	$L_{p,}$ Corley (1966)	$L_{p,}$ Mattock (1967)
f_y, MPa	200	150	80	220	120	60	120	104	163	146	195
	300	100	50	280	160	50	120	104	163	146	195
	488	90	60	240	220	60	120	104	163	146	195
	550	90	50	240	220	60	120	104	163	146	195
z/h,	4.33	90	60	240	220	60	120	104	163	146	195
at h=300mm	6	130	80	260	250	140	140	144	200	152	220
	8	150	70	280	200	140	170	192	245	160	250
	10	200	100	300	270	120	250	240	290	167	280
	12	220	120	350	340	130	240	288	335	175	310
	15	240	130	380	350	150	330	360	403	186	355
d, mm	160	120	70	180	160	120	110	80	115	96	130
at z/h=5	260	100	40	230	210	150	130	120	178	149	205
	360	110	70	340	300	220	180	160	240	201	280
f_c, MPa	30	120	80	220	100	100	100	104	163	146	195
at f_y=488MPa	52	60	60	220	120	120	100	104	163	146	195
	80	40	40	280	120	120	100	104	163	146	195

From the table, numerical results of L_{c2} decreases as f_y and f_c increase while both L_{c2} and L_{ry} increase as z/h and d increase. Similar to existing formulae, L_{ci} is found to be insensitive to f_y and f_c, but closely related to z/h and z. However, L_{rc}, L_{ri} and L_{ci} do not show clear trend of monotonic increasing with z as most of the formulae for L_p do. From the comparisons, L_{ci} shows a good correlation with the empirical plastic hinge length L_p= 0.08z compared to other regions investigated and the cases without confinement yield even closer results. Nevertheless, when z/h is larger than 10, the plastic hinge length tends to be less sensitive to z from numerical study.

6. Conclusions

The work demonstrates that a sophisticated FE model is capable of simulating the complicated behavior in the plastic hinge region of RC beams. This FE model can be used for extensive parametric study of the plastic hinge zone in RC members, from which formulae for the plastic hinge lengths of L_{pc} and L_p can be derived.

Acknowledgements

The work described in this paper was fully supported by a grant from the City University of Hong Kong (Project No. 9231016) and the computational work using commercial software DIANA was supported by the computing facilities provided by ACIM from CityU.

References

[1] Au FTK and Bai ZZ (2007). Two-dimensional nonlinear finite element analysis of monotonically and non-reversed cyclically loaded RC beams. Engineering Structures 2007; 29: 2921–2934

[2] Bae SJ and Bayrak O (2008). Plastic Hinge Length of Reinforced Concrete Columns. ACI Structural Journal, V. 105, No. 3, May-June.

[3] Baker ALL (1956). Ultimate load theory applied to the design of reinforced and prestressed concrete frames. Concrete Publications Ltd., London.

[4] Coleman J and Spacone E (2001). Localization issues in force-based frame elements. Journal of Structural Engineering ASCE; 127(11): 1257–1265.

[5] Comite Euro-International du Beton. Bulletin (1993) D'information no. 213/214 CEB-FIP Model Code 1990 (concrete structures), Lausanne; May 1993

[6] Corley GW (1966). Rotation capacity of reinforced concrete beams. ASCE J. Struct. Div., 92(10), 121–146.

[7] Hines EM, Restrepo JI, and Seible F (2004). Force-displacement characterization of well-confined bridge piers. ACI Structural Journal, V. 101, No. 4, July-Aug. pp. 537-548.

[8] Mander JB, Priestley MJN, Park R and Fellow ASCE (1988). Theoretical stress-strain model for confined concrete. ASCE Journal of Structural Engineering, Vol.114,No.8, August.

[9] Mattock AH (1964). Rotational Capacity of Hinging Regions in Reinforced Concrete Beams. Flexural Mechanics of Reinforced Concrete, SP-12, American Concrete Institute, Farmington Hills, MI, pp. 143-181.

[10] Mattock AH (1965). Rotational capacity of hinging regions in reinforced concrete beams.. American Concrete Institute, Detroit, , Report SP-12143-181

[11]] Mattock AH (1967). Discussion of rotational capacity of reinforced concrete beams by W. D. G. Corley. ASCE J. Struct. Div., 93(2), 519–522.

[12] Panagiotakos TB and Fardis MN (2001). Deformations of reinforced concrete members at yielding and ultimate. ACI Struct. J., 98(2), 135–148.

[13] Park R and Pauly T (1975). Reinforced Concrete Structures. Wiley, New York.

[14] Priestley MJN and Park R (1987). Strength and ductility of concrete bridge columns under seismic loading. ACI Struct. J., 84(1), 61–76.

[15] Paulay T and Priestley MJN (1992). Seismic Design of Reinforced Concrete and Masonry Buildings, John Wiley and Sons, New York, 767 pp.

[16] Sawyer HA (1964). Design of concrete frames for two failure states. Proc., Int. Symp. on the Flexural Mechanics of Reinforced Concrete,ASCE-ACI, 405–431.

[17] Scott RH (1996). Intrinsic mechanisms in reinforced conrete beam-column connection behavior. ACI Structural Journal, V. 93, No. 3, May-June. pp. 1-11.

[18] Sheikh SA and Khoury SS (1993). Confined Concrete Columns with Stubs. ACI Structural Journal, V. 90, No. 4, July-Aug. pp. 414-431.